Reverse optimum safety factor approaches as effective tools for reliability-based topology optimization with application to cementless hollow stems used in total hip replacement

Approches reverses des facteurs de sécurité optimaux en tant qu'outils efficaces pour l'optimisation fiabiliste de topologie avec une application aux tiges creuses sans ciment utilisées dans le remplacement total de la hanche

Ghais Kharmanda [1,2*], Hasan Mulki [3]

[1] Mechanics Laboratory of Normandy, INSA Rouen, St Etienne du Rouvray, France
[2] 3D printing 4U (UG), Cologne, North Rhine-Westphalia, Germany
[3] College of Engineering and Technology, American University of the Middle East, Kuwait City, Kuwait
* Corresponding author: Ghais.Kharmanda@3d-printing-4u.com

ABSTRACT. During the last two decades, the different developments of Reliability-Based Topology Optimization (RBTO) can be divided into two groups. The first group called developments from a point of view 'topology optimization', leading to different layouts with decreasing rigidity (increasing compliance) levels which is considered as a drawback of these methods. In addition, some researchers consider that there is no physical meaning when representing the limit state function by the prescribed volume constraint. However, the second group, being called developments from a point of view 'reliability analysis', often leads to same layouts with increasing rigidity (or decreasing compliance) levels. The single drawback of these methods is to provide the same layouts with different thickness. Some researchers consider that this finding does not represent any importance since a detailed design stage is required to control the structural rigidity. To overcome both drawbacks, Reverse Optimum Safety Factor (ROSF) approaches are presented here to combine the two points of view to generate several layouts with increasing rigidity levels. These strategies are applied to the total hip replacement at the conceptual design stage. This way several types of hollow stems are generated considering the daily loading cases. The ROSF approaches are compared with the previous Inverse Optimum Safety Factor (IOSF) approaches. The results show that despite both approaches leading to several layouts, the ROSF approaches provide layouts with increasing rigidity (or decreasing compliance) levels. In addition to this advantage, the developed approaches lead to a decrease of material quantity in some cases (higher rigidity and less material quantity). The resulting hip stems can be additively manufactured to guarantee the configuration optimality without performing shape and sizing optimization procedures.
KEYWORDS. Deterministic Topology Optimization (DTO), Reliability-Based Topology Optimization (RBTO), Optimum Safety Factor (OSF), Inverse Optimum Safety Factor (IOSF).

1. Introduction

The Reliability-Based Topology Optimization (RBTO) model leads to several solutions with different advantages such as weight reduction [1-4]. The different RBTO developments can be classified in two points of view:

From point of view 'topology optimization', Kharmanda and Olhoff [1] have elaborated an RBTO model with object of providing the designer with several reliability-based structures, however the classical topology optimization produces only a single deterministic topology. It has been shown that the importance of the RBTO model yields structures being more reliable than those produced by deterministic topology optimization (for the same weight, see also [2-4]. In the RBTO model,

reliability constraints have been introduced into deterministic topology optimization problem. The initial step is the sensitivity analysis which is used to show the effect of random variables on the compliance. The objective here is to select the random variables which have a significant influence on the objective function. A Gradient-Based Method (GBM) had been developed where the limit state function was considered as a linear combination of random variables. Using this strategy, two separate steps are considered. The first step is represented by a sensitivity analysis to select the effective random variables, while the second step is to perform the optimization process which itself uses a sensitivity analysis with respect the optimization variables represented by the material densities. Several developments have been next carried out considering the same point of view [5-9]. Among these works, Patel and Choi [5] dealt with this kind of problem considering neural networks which have been efficiently applied on different truss structures. Recently, Meng et al. [10] presented a hybrid method of RBTO to handle epistemic and aleatory uncertainties. It was an efficient single optimization loop method based on Karush–Kuhn–Tucker optimality condition.

From a point of view 'reliability analysis', the classical topology optimization is formulated as finding the stiffest structural layout considering a volume constraint. It had been considered that the feasibility of volume constraint was not critical in structural design problems. It is more important to consider the variations of the stiffness under uncertainties. Bae and Wang [11] were the first who started the developments from point of view 'reliability analysis' by formulating the topology design optimization as volume minimization problem considering a displacement constraint and applied the Reliability-Based Design Optimization (RBDO) technique to maintain the robustness of stiffness in the topology design. Next, Jung et al. [12] extended that to geometrically nonlinear problems. After that, Agarwal [13] employed a decoupled RBDO approach where the topology optimization is separate from the reliability analysis. Next, Patel et al. [14] proposed the gradient free Hybrid Cellular Automata (HCA) method to incorporate uncertainty with respect to material property also. Eom et al. [15] used bi-directional evolutionary structural optimization and the standard response surface method to perform the RBTO model. Finally, a computational RBTO method developed by Jalalpour and Tootkaboni [16] for continuum domains under material properties uncertainty.

Comparing both points of view ('topology optimization' and 'reliability analysis'), RBTO methods from the point of view 'reliability analysis' are inherently computationally expensive because the design variables being related to the topology optimization problem, are considered as random variables. So, an additional required system analysis is carried out at each iteration (double loops), which leads to a large-scale problem [17]. So, the point of view 'topology optimization' seems to be interesting for topology designers, because it provides several reliability-based structures relative to the reliability index changes. It leads to different layout structures while the developments from the point of view 'reliability analysis' leads to same layout structures with different densities that have no sense for the following optimization stages. However, when considering the developments from the point of view 'topology optimization', all produced reliability-based topologies possess lower rigidity levels in function of the reliability index increase [1-4]. There is a strong need to overcome this drawback. In other words, it is vastly desired to provide different layouts with higher rigidity levels when increasing the reliability index values. Thus, Reverse Optimum Safety Factor Approaches are developed in this paper as effective tools to provide more advantages. The procedure of the proposed strategy is to consider the starting point as the failure point and next to seek the optimum solution being more rigid than the failure point. This way the rigidity should increase in function of the reliability index increase and several reliability-based topologies can be obtained. Thus, it can be considered as a combination tool for developing the RBTO from two points of view.

2. Materials and Methods

2.1. *Deterministic Topology Optimization*

The classical topology optimization problems can be classified here in two ways [18]. The first one is called here, Objective-Based Approach (OBA) where the objective is to minimize the structural compliance considering a target ratio decrease of volume V_f^t. This compliance minimization problem is a typical way used in topology optimization [18] which is called OBA. The mathematical formulation of this problem is:

$$\begin{aligned} &\min : C(\mathbf{x}) \\ &s.t.: \frac{V(\mathbf{x})}{V^0} \le V_f^t \end{aligned} \tag{1}$$

where $C(\mathbf{x})$ is the structural compliance and $\mathbf{x}$ is the optimization variables represented by the densities of the used material in each element. Their values should be found in the interval [0,1]. V^0 and $V(\mathbf{x})$ are the initial- and current structural volume values. Conversely, the second one is called here, Performance-Based Approach (PBA) where the objective is to minimize the structural volume considering a target ratio increase of compliance C_f^t. The mathematical formulation of this problem is:

$$\begin{aligned} &\min : V(\mathbf{x}) \\ &s.t.: \frac{C(\mathbf{x})}{C^0} \le 1 + C_f^t \end{aligned} \tag{2}$$

where C^0 represents the initial structural compliance value.

In general, several topology optimization strategies can be used such as SIMP (Solid Isotropic Microstructure with Penalty), homogenization approach [19]. To solve this kind of topology problem, simple techniques such as Optimality Criteria (OC) and the Sequential Convex Programming (SCP) are used here for Formulations 1 and 2, respectively. The OC is carried out solving the optimality conditions directly [20]. The SCP is considered as an extension of the Method of Moving Asymptotes (MMA) which was introduced by [21,22] added a line search procedure. Both methods have been shown their efficiency for large scale problems [23].

2.2. *Reliability Index*

A reliability index β has been introduced to generate several topologies considering transformation between the physical and normalized spaces (Figure 1). This transformation correlates the random variable with its probabilistic model (mean and standard-deviation). This way it is possible to control the different parameters representing the uncertainty. The evaluation of reliability index is carried out using FORM (First Order Reliability Method). The objective is to find the Most Probable failure Point (MPP) by the following optimization procedure [17]:

$$\begin{aligned} &\beta = \min d(\mathbf{u}) \\ &s.t.: H(\mathbf{u}) = 0 \end{aligned} \tag{3}$$

where $H(\mathbf{u}) = 0$ is the limit state function and $\mathbf{u}$ is called the normalized vector represented as the image of the random variable in the normalized space. $d(\mathbf{u})$ is the distance in the normalized space between the limit state and the origin. For a problem of *n* random variables, it is given by:

$$d(\mathbf{u}) = \sqrt{\sum_{i=1}^{n} u_i^2} \tag{4}$$

The reliability analysis is generally carried out using an optimization method to solve problem (3) as in GBM [1-4]. However, when considering the optimality conditions, this problem can be solved analytically considering the basic principle of the IOSF strategies [8]. This principle is used in this work in the next sections with the object of distributing the target reliability index value β_t in a proportional way considering the sensitivities with respect to the random variables. In this case, the random variables can be treated here in macro-structural scales (such as geometrical dimensions), while the design variables are treated in micro-structural scales (such as material densities). Problem (3) is considered in this work for a single failure mode. However, when treating several failure modes, a system reliability analysis should be introduced (the interested reader can refer to [17]).

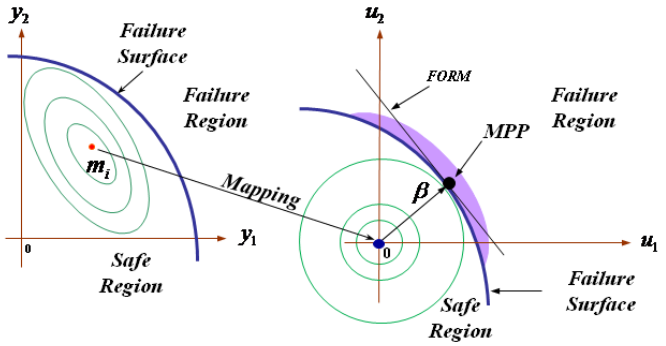

Figure 1. *Transformation image between the physical space and the normalized one.*

2.3. *Reliability-Based Topology Optimization*

A literature review of the different RBTO developments can be found in [24]. Among these methods, Inverse Optimum Safety Factor (IOSF) approaches are selected as effective tools for further developments. According to ISOF approaches, the structural compliance values increase when the values of the reliability index increase. Rationally, when increasing the reliability levels, the structural rigidity should increase (the structural compliance should decrease). When using these approaches, the main findings are represented by providing different layouts. However, the increase of compliance which means decrease of rigidity, represents the drawback of these approaches. Conversely, the objective of the current ROSF approaches is to decrease the structural compliance values when increasing the reliability index values. This fits with the objective of different developments from the point of view of 'reliability analysis'. In addition, it should provide several reliability-based topologies. This fits with the objective of different developments from a point of view 'topology optimization'. In other words, this proposed approach should lead to several layouts with decreasing structural compliance values in function of the reliability index value increase. This way it combines the different developments from both points of view.

2.3.1. *Objective-Based R&IOSF Approaches (OR&OI)*

Considering the Objective-Based Approaches, the problem of RBTO model is to minimize the structural compliance under a target ratio decrease of volume V_f^t and the reliability constraint. In literature, the topology optimization problem which consists of minimizing the structural compliance subject to a prescribed volume fraction is most established [25]. The RBTO problem is then mathematically written as:

$$\begin{aligned} &\min : C(\mathbf{x}) \\ &s.t.: \beta(\mathbf{u}) \geq \beta_t \\ &and : \frac{V(\mathbf{x})}{V^0} \leq V_f^t \end{aligned} \qquad (5)$$

where β_t is the required reliability index to be satisfied. **u** is the normalized vector gathering random variables with its probabilistic model (mean and standard deviation). The failure is generally related to compliance. However, in this method, structural compliance is considered as an objective function. The initial principle of coupling between reliability analysis and topology optimization is carried out considering several simplifications [17]. For example, the reliability analysis being a quantitative of nature can be applied easily to shape and sizing optimization, while due to the qualitative nature of the resulting topology optimization layouts, several simplifications are assumed. One of them is to apply the basic idea of (Optimum Safety Factor) OSF which is represented by distributing of the sum of the absolute values of the failure criterion derivatives with respect to the random variables **y** (a detailed derivation of OSFs can be found in [17]). The resulting partial values represent the effect of each random variable on the failure criterion function. For this methodology, this function is treated as objective function and the same distribution idea is applied. Thus, the sensitivity estimation is carried out for the objective function which is considered as a failure criterion. So, the optimum value of the normalized vector can be written by:

$$u_i^{Opt} = \pm\beta_t \sqrt{\frac{\left|\frac{\partial F}{\partial y_i}\right|}{\sum_{j=1}^{n}\left|\frac{\partial F}{\partial y_j}\right|}} \tag{6}$$

Considering the derivative sign of the objective function with respect to random variables y_i , we write for the Objective-Based IOSF Approach [8]:

$$\frac{\partial F}{\partial y_i} > 0 \Leftrightarrow u_i^{Opt} > 0 \text{ and } \frac{\partial F}{\partial y_i} < 0 \Leftrightarrow u_i^{Opt} < 0 \tag{7}$$

and for the Objective-Based ROSF Approach:

$$\frac{\partial F}{\partial y_i} > 0 \Leftrightarrow u_i^{Opt} < 0 \text{ and } \frac{\partial F}{\partial y_i} < 0 \Leftrightarrow u_i^{Opt} > 0 \tag{8}$$

2.3.2. *Performance-Based R&IOSF Approaches (PR&PI)*

Considering the Performance-Based Approaches, the RBTO problem consists of minimizing the structural volume under the compliance constraint and the reliability one. The RBTO problem is then mathematically written as:

$$\begin{aligned} &\min : V(\mathbf{x}) \\ &s.t. : \beta(\mathbf{u}) \geq \beta_t \\ &and : \frac{C(\mathbf{x})}{C^0} \leq 1 + C_f^t \end{aligned} \tag{9}$$

The optimum value of the normalized vector can be expressed by:

$$u_i^{Opt} = \pm\beta_t \sqrt{\frac{\left|\frac{\partial G}{\partial y_i}\right|}{\sum_{j=1}^{n}\left|\frac{\partial G}{\partial y_j}\right|}} \tag{10}$$

According to the derivative sign of the limit state function with respect to random variables y_i, we write for the Performance-Based IOSF Approach [8]:

$$\frac{\partial G}{\partial y_i} > 0 \Leftrightarrow u_i^{Opt} > 0 \text{ and } \frac{\partial G}{\partial y_i} < 0 \Leftrightarrow u_i^{Opt} < 0 \quad (11)$$

and for the Performance-Based ROSF Approach:

$$\frac{\partial G}{\partial y_i} > 0 \Leftrightarrow u_i^{Opt} < 0 \text{ and } \frac{\partial G}{\partial y_i} < 0 \Leftrightarrow u_i^{Opt} > 0 \quad (12)$$

2.4. *Probabilistic distribution laws*

To apply these approaches, distribution laws should be selected. In this work, the normal distribution is used for the random variable. This way the safety factor can be expressed by:

$$S_{f_i} = 1 + \lambda_i \cdot u_i^* \quad (13)$$

where λ_i represents the relationship between the mean value μ_i of the random variable y_i and its standard-deviation σ_i as follows:

$$\lambda_i = \sigma_i / \mu_i \quad (14)$$

Here, the starting point is considered as the failure point P_y^* and an RBTO layout P_x^* is next obtained. This point P_x^* must meet a target reliability index β_t. The DTO procedure is utilized to reach the failure point P_y^*.

2.5. *Total hip replacement*

To obtain the optimum hollow stems utilized in the total hip replacement, topology optimization can be performed to provide a suitable initial topology. To meet the different patient specifications, the RBTO is used to provide several layouts of the hollow stems. In this work, 3D and 2D stem models implanted in bone tissues are elaborated to test the different approaches.

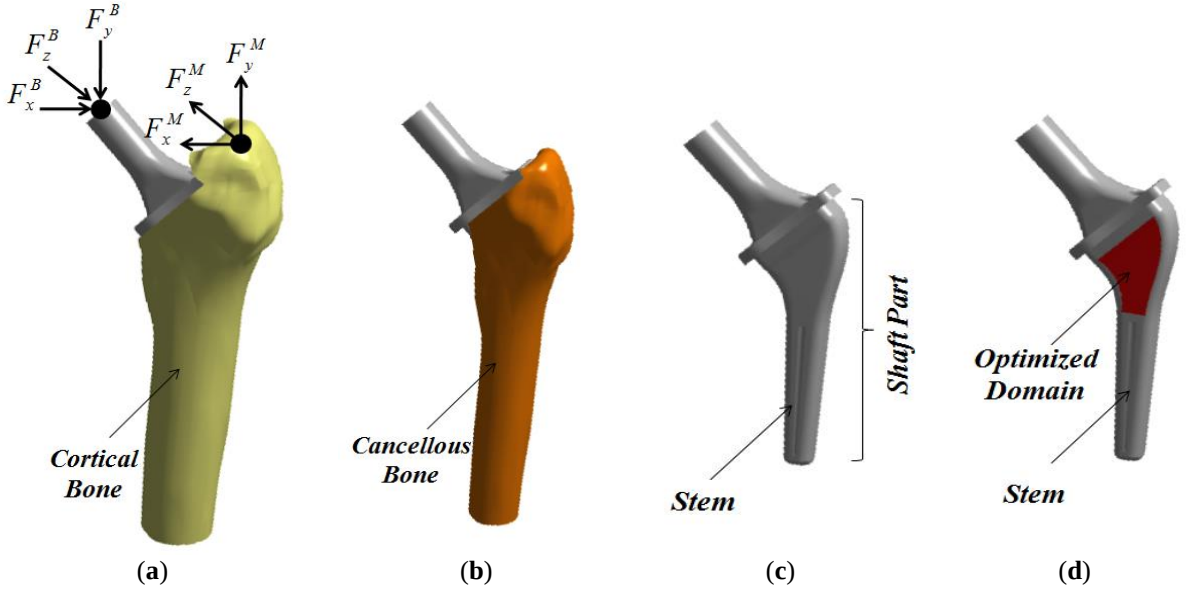

Figure 2. *(a) 3D model stem implanted in bone tissues with the applied forces, (b) Stem with the cancellous tissue, (c) Stem considering its whole body as an optimized domain, and (d) Stem considering the inner volume as an optimized domain.*

2.5.1. *3D modeling*

Figure 2a shows the studied 3D model stem implanted in the cortical and cancellous bone tissues and the applied body and muscle forces ($\mathbf{F}^B$ and $\mathbf{F}^M$). Figure 2b shows the studied 3D stem with the cancellous bone tissue.

In this study, three cases of loading are considered: L1:one-legged stance, L2: ab-duction, and L3: adduction. Their different component values in three directions (F_x^B , F_y^B, F_z^B, F_x^M , F_y^M and F_z^M) are found in Table 1 [26].

Loading Cases		F_x **[N]**	F_y **[N]**	F_z **[N]**
L1	$\mathbf{F}^B$	224	-2246	-972
	$\mathbf{F}^M$	-768	1210	726
L2	$\mathbf{F}^B$	-136	-1692	-630
	$\mathbf{F}^M$	-166	957	382
L3	$\mathbf{F}^B$	-457	-1707	-796
	$\mathbf{F}^M$	-383	547	669

Table 1. *Applied body and muscle forces [26].*

To perform 3D topology optimization using, GENESIS being a powerful topology software is coupled to the ANSYS Workbench software. In addition, a multiple loading feature implemented in ANSYS Workbench is used to show the effect of the three loading cases. When performing the topology optimization, two different optimized domains are treated. The first model is to consider the whole stem as an optimized domain as shown in Figure 2c. In fact, the topology optimization algorithm allows us to delete un-needed regions especially at the border which is in contact with the bone tissue. This may affect the stem shape and then its performance. This way the outer border should not considered as optimization domain. The optimized and non-optimized regions should be specified at the shaft of the studied stem. So, the second model is to consider the inner region as an optimized domain as illustrated in Figure 2d. The whole structure is fixed at the lower side at the lower area of the cortical and cancellous bone tissues.

2.5.2. *2D modeling*

Figure 3a shows the studied 2D stem model implanted in the cortical and cancellous bone tissues and the applied body and muscle forces ($\mathbf{F}^B$ and $\mathbf{F}^M$). Their different component values in two directions (F_x^B , F_y^B, F_x^M and F_y^M) are found in Table 2 [27].

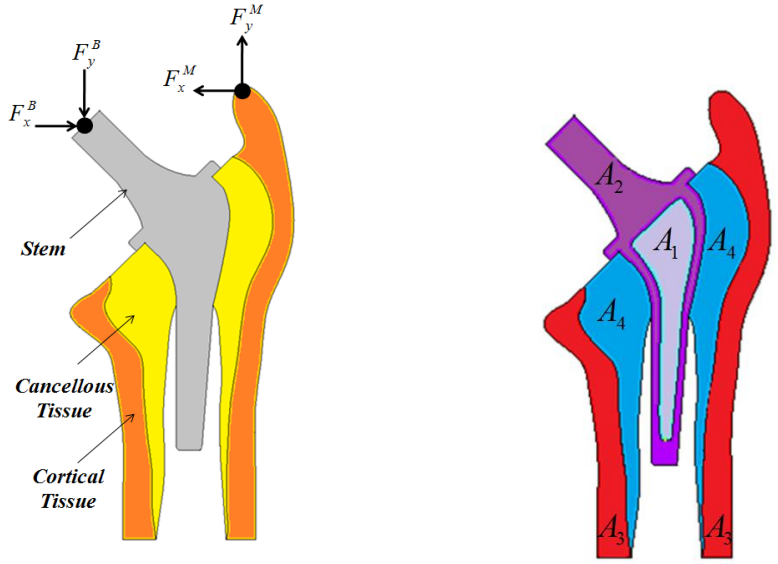

(**a**) (**b**)

Figure 3. *a) studied 2D stem model implanted in bone tissues with applied loads and b) Inner area as an optimized domain.*

Figure 3b shows the different areas to be specified as optimized or non-optimized domains. The inner area of the shaft A_1 is assumed to be the optimized domain, while the other areas to be non-optimized domains: A_2 contains the head, neck, shoulder and an outer area of the shaft, A_3 contains the cortical tissue and A_4 contains the cancellous tissue. The total numbers of elements and nodes are 1782 and 5733, respectively. The used element is called PLANE82 (nonlinear, 8 nodes). The contact between the different layers is assumed to be rigid. The used meshing technique is called smart size which can be adopted according to the geometry complexity.

Loading Cases		F_x **[N]**	F_y [N]
L1	$\mathbf{F}^B$	942	2117
	$\mathbf{F}^M$	330	621
L2	$\mathbf{F}^B$	-2997	1119
	$\mathbf{F}^M$	-49	348
L3	$\mathbf{F}^B$	1283	866
	$\mathbf{F}^M$	268	383

Table 2. *Applied body and muscle forces.*

For 2D and 3D models, all used materials are considered homogeneous and linear elastic. The cortical bone tissue is assumed to be isotropic with Young's modulus $E = 17$ GPa and Poisson's ratio $\nu = 0.33$. The cancellous bone tissue is also assumed to be iso-tropic material with Young's modulus MPa and Poisson's ratio [28]. The stem is made of titanium alloy with Young's modulus $E = 110$ GPa and Poisson's ratio: $\nu = 0.3$ [29].

3. Results and Discussion

The DTO is carried out for the 3D and 2D models, however the RBTO is performed only for 2D model. For the RBTO, the different developments are implemented considering the APDL (ANSYS Parametric Design Language) where several commends can be used to deal with the new developments. The cross section of the current 2D model is selected to be like a previous configuration modeled by Kharmanda [28].

3.1. *Results for 3D model*

The different layouts are represented by a color scale where the colors present the materials densities. The red color means an element with full material which can be represented by a solid element. The colors change according to the density to become blue which can be represented by a void element. The topology optimization is first applied to 3D models. Figures 4a and b show the front and back views of the resulting topologies when considering the whole stem as an optimized domain. In this case, the resulting configuration at the conceptual design stage may affect the whole performance of the stem which may lead to a difficulty of fixation when drilling the bone. Therefore, the inner geometry is considered to increase the osseointegration. Figures 4c and d show the front and back views of the resulting topologies when considering the inner region stem as an optimized domain.

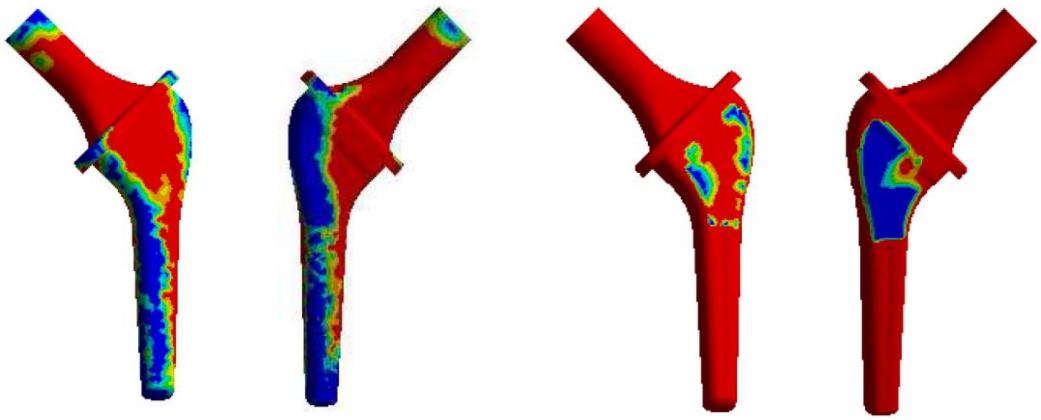

(**a**) (**b**) (**c**) (**d**)

Figure 4. *a) Front and (b) back views for the resulting topologies when considering the whole stem as an optimized domain, (c) Front and (d) back views for the resulting topologies when considering the inner region stem as an optimized domain*

The 3D application leads to configurations that are too complex to be efficiently analyzed. This way the responses such as stresses will not be homogenous along the stem hole. Thus, a simplified 2D model is necessary to integrate the DTO and RBTO into the total hip replacement at the conceptual design stage to sketch several types of hollow stems.

3.2. *Results for 2D model*

DTO and RBTO models are considered here to compare the developed approaches for the three daily loading cases L1, L2 and L3. The reliability index values belong to the interval $\beta \in [3-4.25]$. Three values are selected to identify the effect of the layout changes: β =3, 3.8 and 4.25. The given material properties (see Subsection 2.5.2.), the forces (see Table 2) and boundary limitations ($V_f^t = 50\%$ and $C_f^t = 50\%$) are considered as data for the starting point. The standard-deviation is considered proportional to the mean values (starting point) to be 10% ($\lambda_i = 0.1$, see Equation (13)). Two topology optimization methods implemented in ANSYS software are used: Optimality Criteria

(OC) and Sequential Convex Programming (SCP). Table 3 shows the different numerical results for the DTO and the RBTO using Objective-Based R&IOSF Approaches for three loading cases: L1, L2 and L3.

Case & Model.		*DTO*	*RBTO*					
			OI			*OR*		
			β =3	β =3.8	β =4.25	β =3	β =3.8	β =4.25
L1	*Com*	0.74	0.95	1.01	1.05	0.61	0.56	0.48
	Vol	351.37	321.77	313.88	309.43	380.98	388.87	407.44
L2	*Com*	0.72	0.85	0.91	0.93	**0.56**	**0.51**	**0.49**
	Vol	351.38	383.62	392.22	397.06	**319.13**	**310.53**	**305.69**
L3	*Com*	0.37	0.77	0.91	1.01	0.16	0.13	0.12
	Vol	351.38	307.89	296.30	289.78	394.86	406.46	412.98

Table 3. *Numerical DTO and RBTO results.*

Table 4 shows the different numerical results for the DTO and the RBTO using Performance-Based R&IOSF Approaches for three loading cases: L1, L2 and L3.

Case & Model		*DTO*	*RBTO*					
			PI			*PR*		
			β =3	β =3.8	β =4.25	β =3	β =3.8	β =4.25
L1	*Com*	1.07	1.97	2.28	2.45	0.53	0.43	0.39
	Vol	149.66	89.96	85.03	85.85	218.82	229.89	248.78
L2	*Com*	0.95	1.04	1.07	1.08	0.87	0.84	0.82
	Vol	107.22	132.39	134.24	134.12	112.59	115.68	121.71
L3	*Com*	0.48	0.94	1.10	1.20	**0.22**	**0.18**	**0.17**
	Vol	264.70	253.94	249.72	246.30	**261.70**	**254.73**	**264.09**

Table 4. *Numerical DTO and RBTO results.*

Table 5 shows the different sensitivity results for the OBA and the PBA considering the three loading cases: L1, L2 and L3. The used sensitivity method is the central finite difference method which is considered as an accurate method [17].

Parameters	L1		L2		L3	
	OBA	PBA	OBA	PBA	OBA	PBA
F_x^B	-1.65×10^{-2}	-6.38×10^{-3}	1.33×10^{-3}	-1.41×10^{-2}	7.93×10^{-3}	1.09×10^{-2}
F_y^B	1.52×10^{-2}	1.34×10^{-2}	9.58×10^{-3}	1.32×10^{-2}	-7.23×10^{-4}	-1.82×10^{-3}
F_x^M	-2.25×10^{-3}	-2.83×10^{-3}	1.00×10^{-2}	1.25×10^{-2}	-7.14×10^{-3}	-9.98×10^{-3}
F_y^M	-2.42×10^{-3}	-8.86×10^{-5}	-1.04×10^{-3}	7.19×10^{-5}	-2.27×10^{-4}	-3.69×10^{-4}
E^{Metal}	-7.04×10^{-6}	-9.58×10^{-6}	-7.37×10^{-6}	-8.14×10^{-6}	-3.34×10^{-6}	-4.35×10^{-6}
$E^{Cortical}$	-4.90×10^{-6}	-5.76×10^{-6}	-1.02×10^{-6}	-7.44×10^{-6}	-5.64×10^{-6}	-7.87×10^{-6}
$E^{Cancellous}$	3.24×10^{-4}	2.10×10^{-4}	-1.93×10^{-4}	2.29×10^{-4}	2.53×10^{-4}	3.41×10^{-4}
ν^{Metal}	-2.14×10^{-1}	0	2.50×10^{-2}	1.07×10^{-1}	0	0
$\nu^{Cortical}$	-4.55×10^{-4}	0	7.42×10^{-3}	-1.11×10^{-1}	0	0
$\nu^{Cancellous}$	1.52×10^{-4}	0	-1.52×10^{-3}	7.73×10^{-3}	0	0
V_f^t / C_f^t	2.15×10^{-2}	7.01×10^{-3}	-5.79×10^{-3}	5.78×10^{-3}	3.34×10^{-3}	3.23×10^{-3}

Table 5. *Compliance sensitivity results with respect to eleven random variables*

3.2.1. *Case L1*

3.2.1.1. Case L1 using Objective-Based R&IOSF Approaches

For the first loading case L1, Figure 5a shows the DTO layout considering the structural compliance as an objective function [30]. Figures 5b, c and d show the RBTO layouts when using Objective-Based IOSF Approach for $\beta=3$, $\beta=3.8$ and $\beta=4.25$ [30], respectively. Figures 5e, f and g show the RBTO layouts when using Objective-Based ROSF Approach for $\beta=3$, $\beta=3.8$ and $\beta=4.25$.

As shown in Figure 5 for L1, both approaches (Objective-Based R/IOSF Approaches) do not lead to a significant layout change even when arriving to the end of the interval ($\beta=4.25$).

3.2.1.2. Case L1 using Performance-Based R&IOSF Approaches

For the first loading case L1, Figure 6a shows the DTO layout considering the structural compliance as a performance function [30]. Figures 6b, c and d show the RBTO layouts when using Performance-Based IOSF Approach for $\beta=3$ [30], $\beta=3.8$ and $\beta=4.25$, respectively. Figures 6e, f and g show the RBTO layouts when using Performance-Based ROSF Approach for $\beta=3$, $\beta=3.8$ and $\beta=4.25$.

As shown in Figure 6 for L1, the Performance-Based ROSF Approaches leads to a significant change when the reliability index is: $\beta=3.8$ (Figure 6f). However, the Performance-Based IOSF Approaches does not lead to a significant change even when reaching the end of the interval where the reliability index is: $\beta=4.25$.

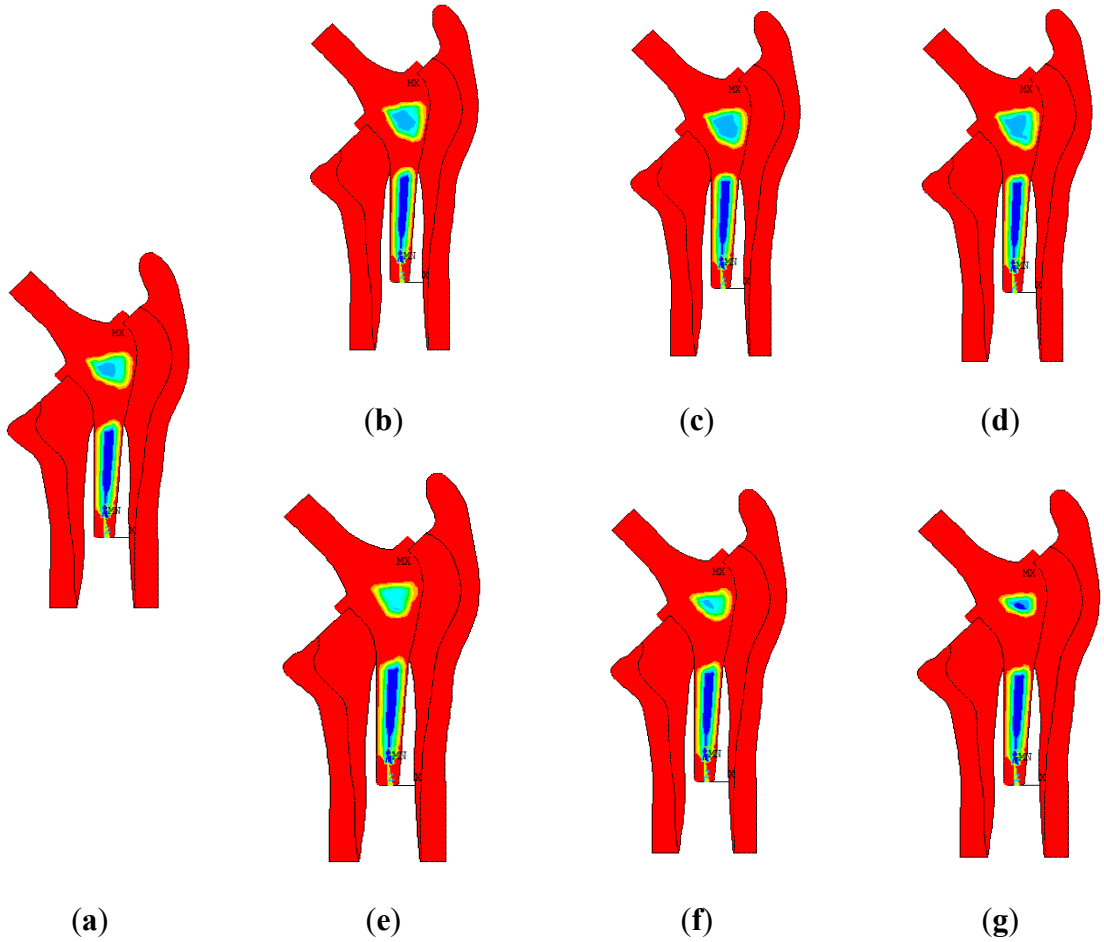

Figure 5. *(a) DTO layout considering the structural compliance as an objective function [30], and RBTO layouts when using Objective-Based IOSF Approach, (b)* $\beta = 3$*, (c)* $\beta = 3.8$ *and (d)* $\beta = 4.25$ *[30], RBTO layouts when using Objective-Based ROSF Approach, (e)* $\beta = 3$*, (f)* $\beta = 3.8$*, and (g)* $\beta = 4.25$ *for the first loading case L1*

Figure 7 shows the structural compliance and volume change in function of reliability index for the different approaches when considering the first loading caseL1. For the Objective-Based strategies, when increasing the reliability index values, the structural compliance increases, while the structural volume decreases for the Objective-Based IOSF Approach. However, when increasing the reliability index values, the structural compliance decreases, while the structural volume increases for the Objective-Based ROSF Approach. Considering the DTO and the RBTO when $\beta = 4.25$, the structural compliance decreases very highly by almost two and half times, while the structural volume increases only by almost 65%. For the Performance-Based strategies, when increasing the reliability index values, the structural compliance increases, while the structural volume decreases for the Performance-Based IOSF Approach. However, when increasing the reliability index values, the structural compliance decreases, while the structural volume increases for the Performance-Based ROSF Approach.

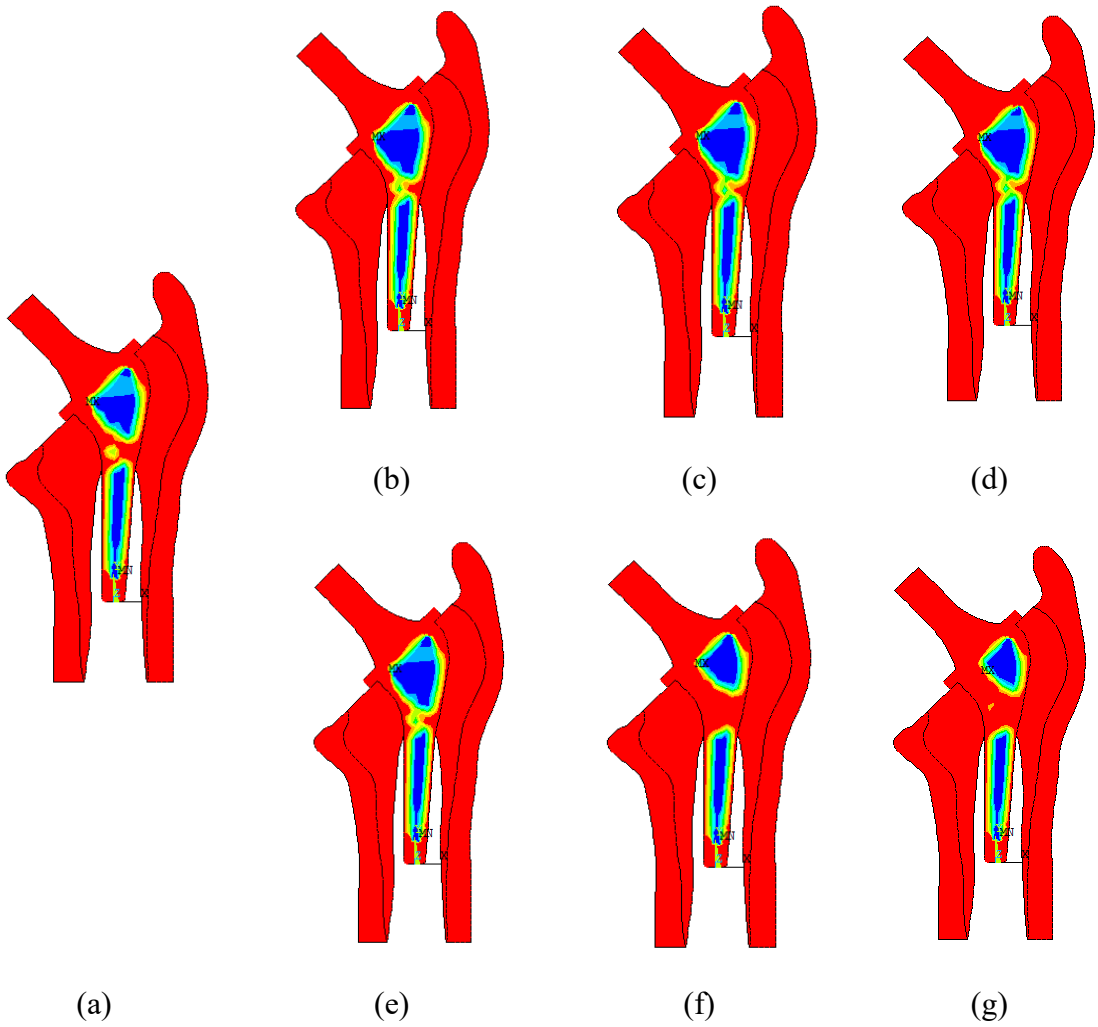

Figure 6. *(a) DTO layout considering the structural compliance as a performance function ([30] and RBTO layouts when using Performance-Based IOSF Approach, (b) $\beta = 3$ [30], (c) $\beta = 3.8$ and (d) $\beta = 4.25$, RBTO layouts when using Performance-Based ROSF Approach, (e) $\beta = 3$, (f) $\beta = 3.8$, and (g) $\beta = 4.25$ for the first loading case L1.*

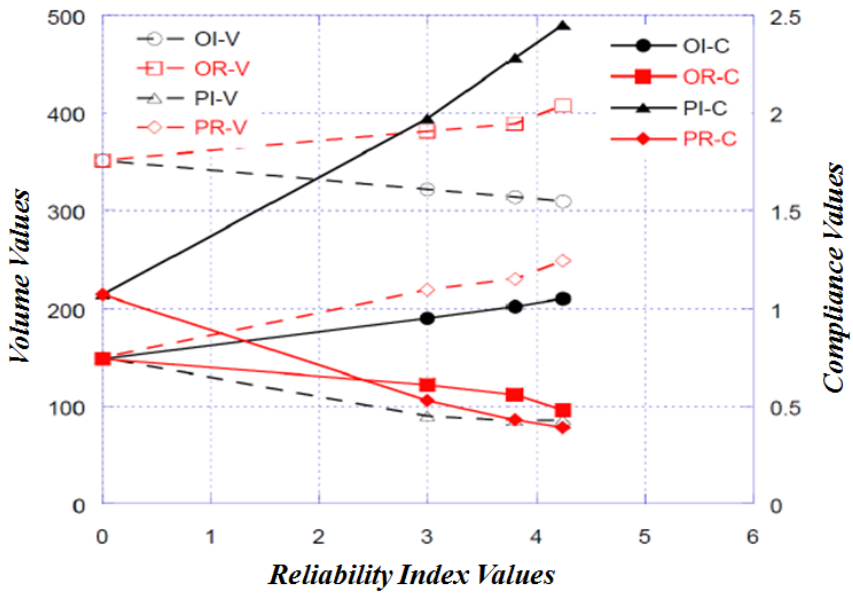

Figure 7. *Structural compliance and volume change in function of reliability index for L1.*

3.2.2. *Case L2*

3.2.2.1. Case L2 using Objective-Based R&IOSF Approaches

For the second loading case L2, Figure 8a shows the DTO layout considering the structural compliance as an objective function [30]. Figures 8b, c and d show the RBTO layouts when using Objective-Based IOSF Approach for $\beta = 3$, $\beta = 3.8$ [30] and $\beta = 4.25$, respectively. Figures 8e, f and g show the RBTO layouts when using Objective-Based ROSF Approach for $\beta = 3$, $\beta = 3.8$ and $\beta = 4.25$.

As shown in Figure 8 for L2, the Objective-Based IOSF Approach leads to a significant layout change when the reliability index is: $\beta = 3.8$. However, the Objective-Based ROSF Approach leads to different layouts especially when the reliability index is: $\beta = 3.8$.

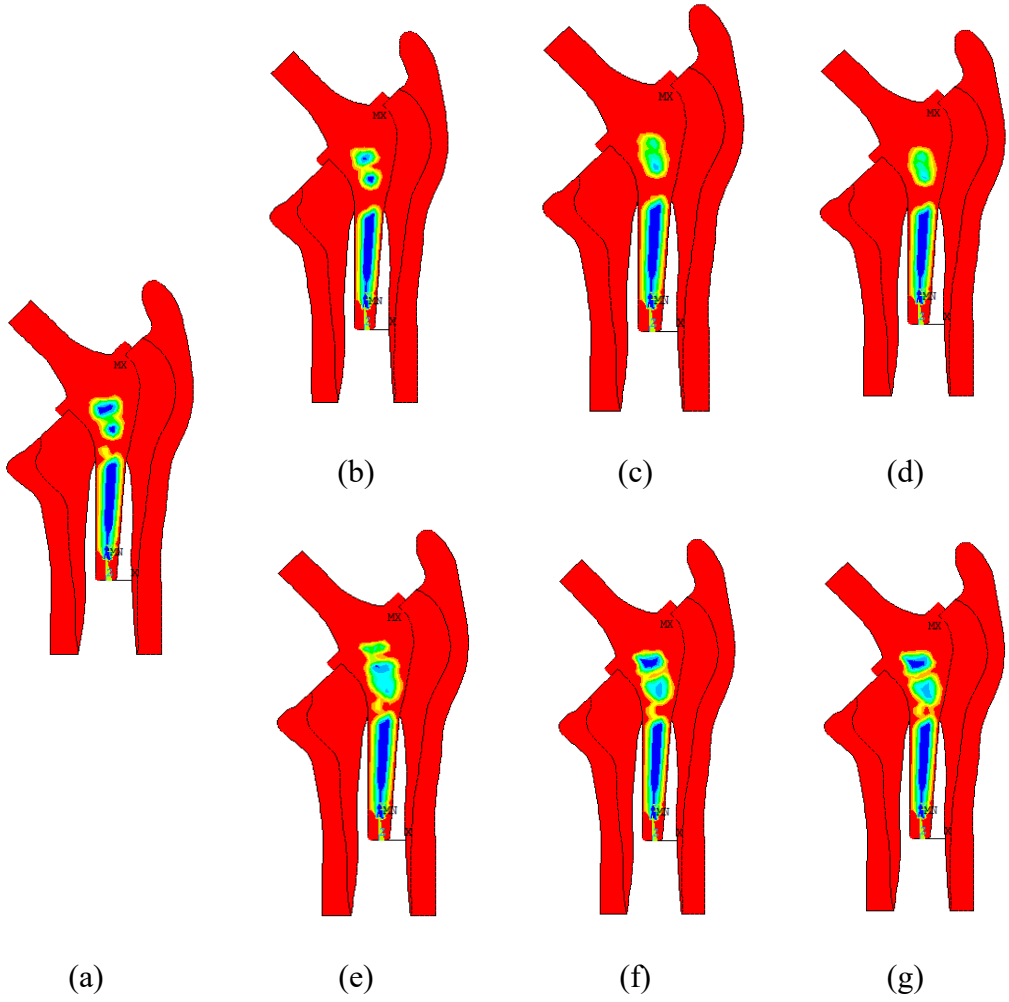

Figure 8. *a) DTO layout considering the structural compliance as an objective function [30], and RBTO layouts when using Objective-Based IOSF Approach, b)* $\beta = 3$, *c)* $\beta = 3.8$ *[30] and d)* $\beta = 4.25$, *RBTO layouts when using Objective-Based ROSF Approach, e)* $\beta = 3$, *f)* $\beta = 3.8$, *and g)* $\beta = 4.25$ *for the second loading case L2*

3.2.2.2. Case L2 using Performance-Based R&IOSF Approaches

For the second loading case L2, Figure 9a shows the DTO layout considering the structural compliance as a performance function [30]. Figures 9b, c and d show the RBTO layouts when using Performance-Based IOSF Approach for $\beta = 3$, $\beta = 3.8$ and $\beta = 4.25$ [29], respectively. Figures 9e, f and g show the RBTO layouts when using Performance-Based ROSF Approach for $\beta = 3$, $\beta = 3.8$ and $\beta = 4.25$.

As shown in Figure 9 for L2, both approaches (Performance-Based R/IOSF Approaches) do not lead to a significant layout change even when arriving at the end of the interval ($\beta = 4.25$).

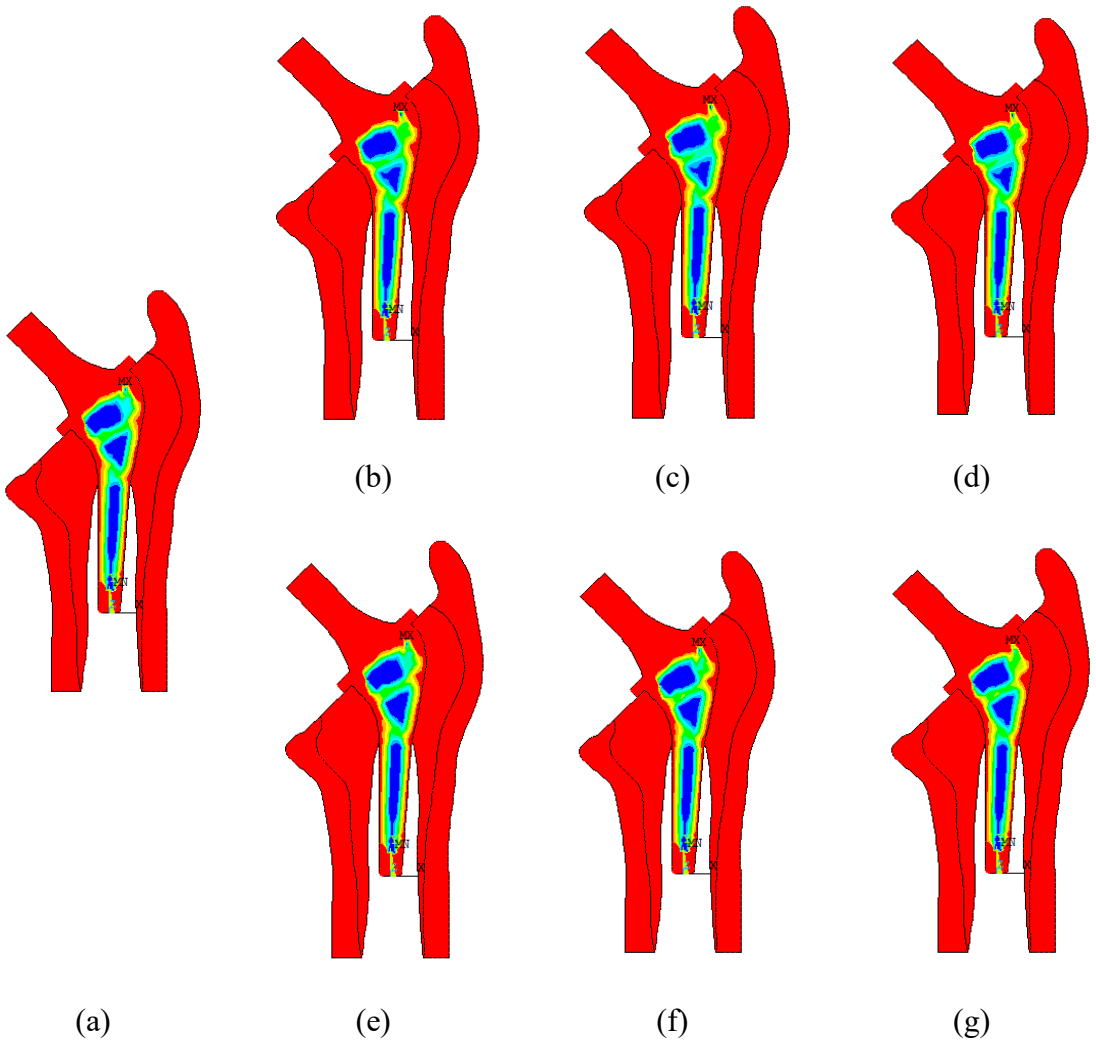

Figure 9. *a) DTO layout considering the structural compliance as a performance function [30], and RBTO layouts when using Performance-Based IOSF Approach, b)* $\beta = 3$, *c)* $\beta = 3.8$ *and d)* $\beta = 4.25$ *[30], RBTO layouts when using Performance-Based ROSF Approach, e)* $\beta = 3$, *f)* $\beta = 3.8$ *and g)* $\beta = 4.25$ *for the second loading case L2*

Figure 10 shows the structural compliance and volume change in function of reliability index for the different approaches when considering the second loading case L2. For the Objective-Based strategies, when increasing the reliability index values, the structural compliance and volume increase for the Objective-Based IOSF Approach. However, when increasing the reliability index values, the structural compliance and volume decrease for the Objective-Based ROSF Approach. For the Performance-Based strategies, when increasing the reliability index values, the structural compliance and volume increase for the Performance-Based IOSF Approach. However, when increasing the reliability index values, the structural compliance and volume decrease for the Performance-Based ROSF Approach. This result shows a big advantage of the proposed method since it leads to light and rigid structures when increasing the reliability levels.

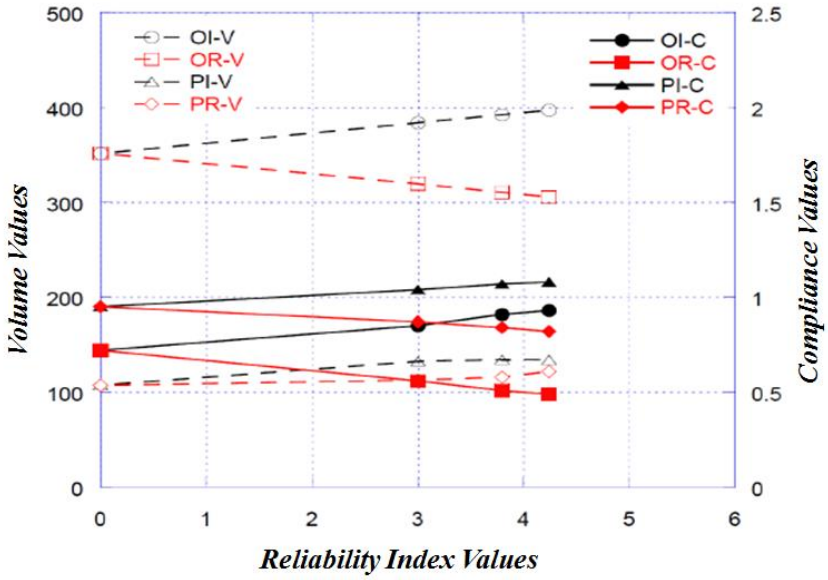

Figure 10. *Structural compliance and volume change in function of reliability index for L2.*

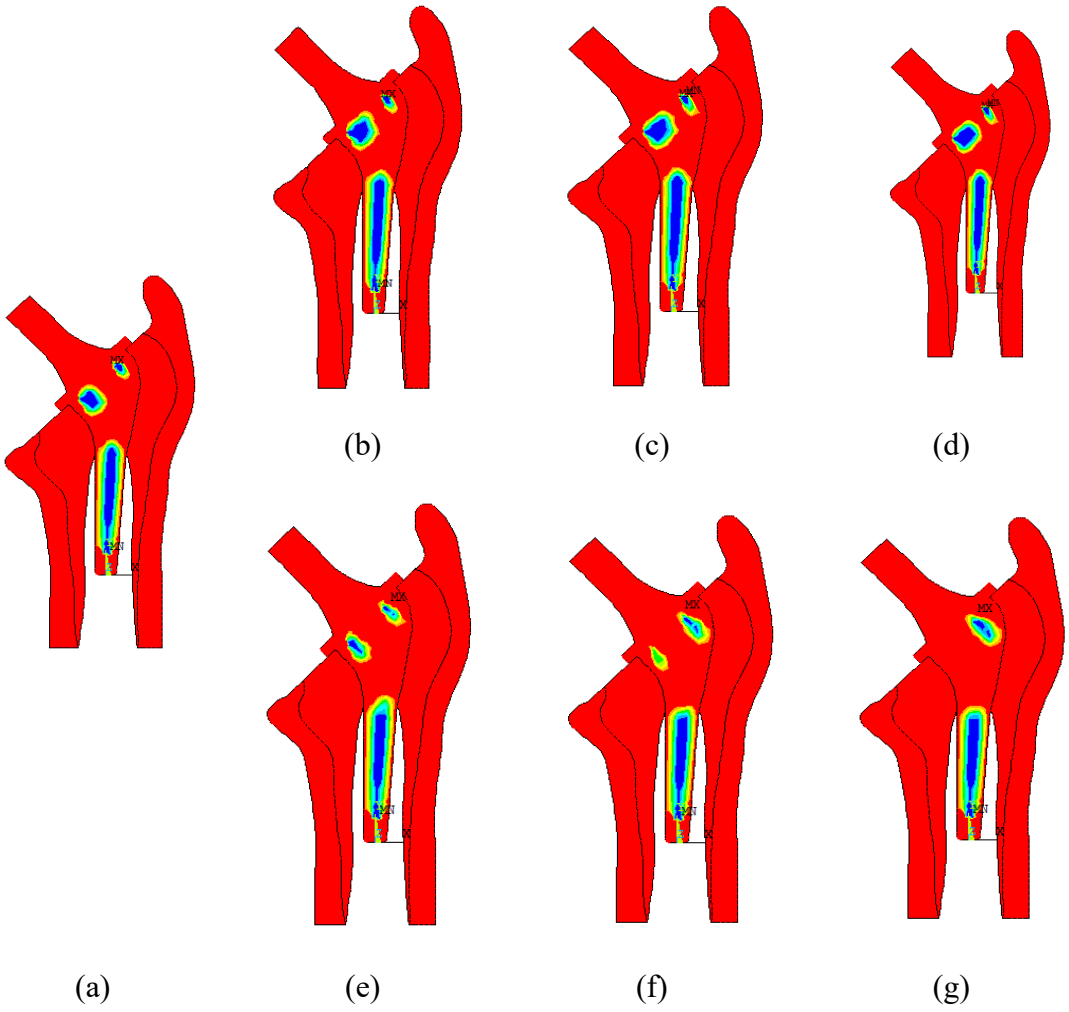

Figure 11. *a) DTO layout considering the structural compliance as an objective function [30], and RBTO layouts when using Objective-Based IOSF Approach, b)* $\beta = 3$*, c)* $\beta = 3.8$ *and d)* $\beta = 4.25$ *[30], RBTO layouts when using Objective-Based ROSF Approach, e)* $\beta = 3$*, f)* $\beta = 3.8$ *and g)* $\beta = 4.25$ *for the third loading case L3.*

3.2.3. *Results for Case L3*

3.2.3.1. Case L3 using Objective-Based R&IOSF Approaches

For the third loading case L3, Figure 11a shows the DTO layout considering the structural compliance as an objective function [30]. Figures 11b, c and d show the RBTO layouts when using Objective-Based IOSF Approach for $\beta = 3$, $\beta = 3.8$ and $\beta = 4.25$ [30], respectively. Figures 11e, f and g show the RBTO layouts when using Objective-Based ROSF Approach for $\beta = 3$, $\beta = 3.8$ and $\beta = 4.25$.

As shown in Figure 11 for L3, the Objective-Based ROSF Approaches) lead to a different layout when the reliability index is: $\beta = 4.25$.

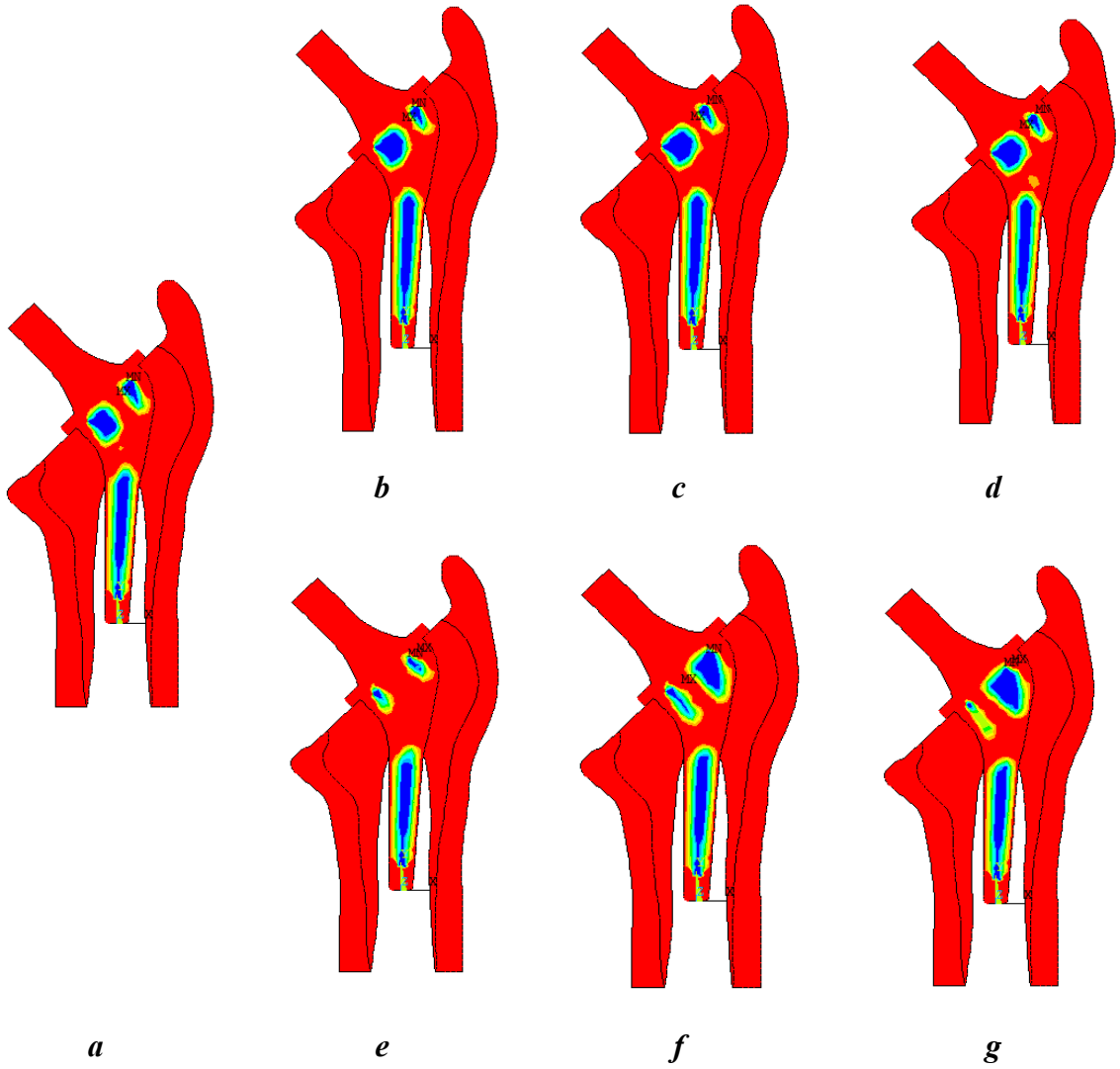

Figure 12. *a) DTO layout considering the structural compliance as a performance function [30], and RBTO layouts when using Performance-Based IOSF Approach, b)* $\beta = 3$*, c)* $\beta = 3.8$ *and d)* $\beta = 4.25$ *[30], RBTO layouts when using Performance-Based ROSF Approach, e)* $\beta = 3$*, f)* $\beta = 3.8$ *and g)* $\beta = 4.25$ *for the third loading case L3.*

3.2.3.2. Case L3 using Performance-Based R&IOSF Approaches

For the third loading case L3, Figure 12a shows the DTO layout considering the structural compliance as a performance function [30]. Figures 12b, c and d show the RBTO layouts when using Performance-Based IOSF Approach for $\beta = 3$, $\beta = 3.8$ and $\beta = 4.25$ [30], respectively. Figures 12e, f and g show the RBTO layouts when using Performance-Based ROSF Approach for $\beta = 3$, $\beta = 3.8$ and $\beta = 4.25$.

As shown in Figure 12 for L2, both approaches (Performance-Based R/IOSF Approaches) lead to a small difference in the resulting layouts when arriving to the end of the interval ($\beta = 4.25$).

Figure 13 shows the structural compliance and volume change in function of reliability index for the different approaches when considering the third loading case L3. For the Objective-Based strategies, when increasing the reliability index values, the structural compliance increases, while the structural volume decreases for the Objective-Based IOSF Approach. However, when increasing the reliability index values, the structural compliance decreases, while the structural volume increases for the Objective-Based ROSF Approach. For the Performance-Based strategies, when increasing the reliability index values, the structural compliance increases, while the structural volume decreases for the Performance-Based IOSF Approach. However, when increasing the reliability index values, the structural compliance decreases, while the structural volume increases for the Performance-Based ROSF Approach. This result also shows a big advantage of the proposed method since it leads to light and rigid structures when increasing the reliability levels until $\beta = 3.8$.

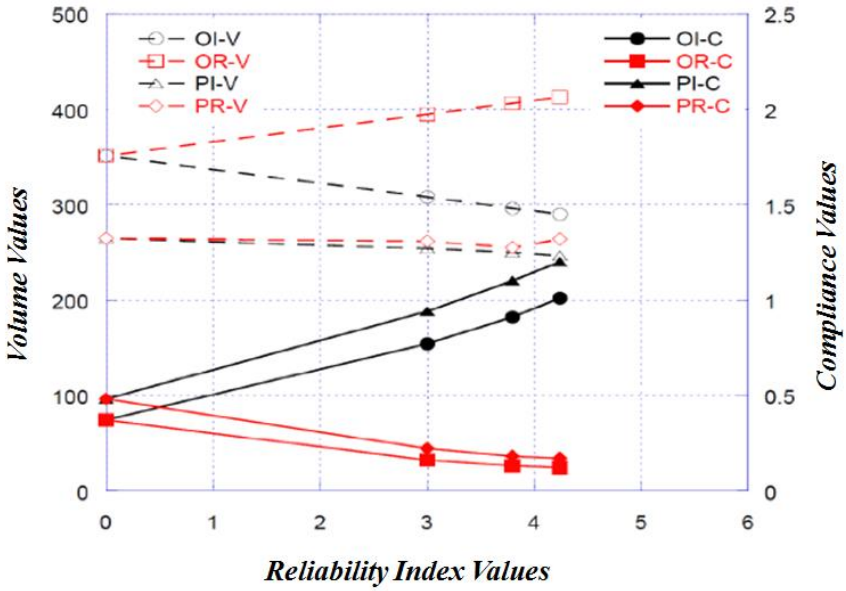

Figure 13. *Structural compliance and volume change in function of reliability index for L3.*

As shown in Tables 3 and 4, the Objective-Based ROSF Approach and the Performance-Based ROSF Approach do not reduce only the structural compliance but the structural volume in Case L2 and L3, respectively. This way new layouts are generated with higher rigidity levels and lower material quantities.

When considering the DTO solutions (Tables 3 and 4) for all loading cases (L1, L2 and L3), the Performance-Based Approach leads to higher values for the structural compliance and lower values of the structural volume relative to the Objective-Based Approach. In addition, it is shown that Performance-Based R&IOSF Approaches are much more sensitive to the reliability index changes than the Objective-Based R&IOSF Approaches.

For a simple topology optimization problem, when considering the OBA (Problem 1) and PBA (Problem 2) for the same given design space, two solutions can be obtained. The OBA problem represented by the minimization of compliance for a prescribed volume fraction, is the most established way in literature [25]. Therefore, the first RBTO model by GBM was associated to the OBA [1] and led to several solutions (only one category of solutions), not only two solutions. Reliability is next integrated into both approaches (OBA/PBA) using IOSF and led to two categories of solutions [8]. However, in this work, two directions of categories are generated: OBA/PBA using

IOSF and ROSF. Each direction has two different categories of solutions regarding the resulting layouts and the output parameters changes (compliance and volume) in function of re-liability index. As shown in Tables 3 and 4, for the first direction of categories (OBA/PBA using IOSF), the compliance values increase when increasing the reliability index values, while it is not the same for the second direction of categories (OBA/PBA using ROSF). An extension of other nonlinear distribution laws will be integrated in the future works to compare the effect of the resulting layouts and output parameters for both directions.

The uncertainty is applied here only to material properties, loads and constraint boundaries where the corresponding sensitivity results are provided in Table 5. The different information can be obtained by using this table and the starting point data and Equations from (6) to (8) and from (10) to (14). In certain cases, there is no effect for Poisson's ratio where the sensitivity values are zeros, while they have a significant influence in other cases. Therefore, it is not recommended to ignore the role of all parameters.

6. Future works and perspectives for RBTO approaches

In general, the non-uniqueness of the resulting topologies is a big concern where many different structures can be found to be local optima for a given problem formulation. This is a fundamental challenge in non-convex optimization, which is the case for almost all structural optimizations. This is a challenge because even selecting a strategy for initial guesses would result in new local optima. Similar to the problem of selecting an initial distribution, it makes the new designs as a function of selecting strategy [31]. Therefore, there is a need to find a suitable strategy to control these guesses. The RBTO approaches generate several topologies considering the reliability index as a reference to control the resulting topology. The developed RBTO approaches in this work allow to control the resulting topologies considering the different used functions (objective and constraints). When comparing the different findings in this work with to our previous one [32], the resulting reliability-based topologies here have higher rigidity and less material quantity in certain cases, which can be considered as a new advantage of the use of RBTO approaches. In addition, a sensitivity study in [32] showed a big influence of the geometrical parameters on the structural compliance (rigidity) for the used 2D bicycle frame structure. So, the geometry uncertainty of hip stems should be included to study the possibility of providing different layouts with a significant difference. This can improve the final layouts in order to meet the different patient specifications. The benefit of this finding can be used in additive manufacturing, especially for medical applications where complex geometries should be considered. Here, a suitable distribution of support structures should be considered to deal with overhanging features [33,34]. The developed RBTO approaches generate several types of support structures with different advantages without using designer’s experience to change the initial design. Furthermore, topology optimization techniques can be used in cellular structure applications which are elaborated for orthopedic scaffolds due to their low elastic modulus values, high compressive strength, etc. [35]. The use of the developed RBTO approaches allows to provide the best compromise between their weight and rigidity. When developing the RBTO approaches for this area, the applications to cellular structures can be extended to cover surgical operations in dentistry (maxilla and mandible) [36]. A cellular structure can be optimized to be used between the fracture’s surfaces to replace the lost bone part considering the advanced strategies in RBTO model. For more advanced applications, several recent developments at micro and macro levels can be found in [24].

5. Conclusion

Two RBTO approaches, called Objective-Based ROSF Approach and Performance-Based ROSF Approach, are presented in this work and applied to design of hip stems. They combine the objective of certain RBTO developments during two decades from two points of view in generating several

layouts with an increasing rigidity level in function of reliability index increase. The application of these methods is carried out to the total hip replacement to provide several kinds of hollow stems. The application to the 3D stem model does not lead to realistic configurations due to 3D loading distribution. Thus, the application to a simplified 2D stem model is obligatory to test the different approaches. The uncertainty is applied on the material properties, loads and constraint boundaries. Significant results are found in the context of generating several reliability-based topologies with increasing rigidity in function of reliability index increase. In some cases, this advantage becomes bigger when obtaining reliability-based topologies with higher rigidity and less material quantity. It is very important to consider the uncertainty on the stem geometry to show the effect of the developed approaches. The application of these developed RBTO strategies to the hollow stems allows us to increase the probability of osseointegration which can occur here in two ways. The first way is to obtain traversal holes where simple sizing and shape optimization are needed to get the detailed design. However, the second one is to obtain porous structures (foams). This way the resulting layouts can be manufactured using additive manufacturing technology. It is recommended to perform a gait cycle simulation at the detailed design stage considering realistic input data (loads, material properties ...) to select the most reliable stem.

List of abbreviations:

APDL	ANSYS Parametric Design Language
DTO	Deterministic Topology Optimization
FORM	First Order Reliability Method
GBM	Gradient-Based Method
HCA	Hybrid Cellular Automata
IOSF	Inverse Optimum Safety Factor
MMA	Method of Moving Asymptotes
MPP	Most Probable failure Point
OBA	Objective-Based Approach
OC	Optimality Criteria
OI	Objective-Based IOSF Approach
OR	Objective-Based ROSF Approach
OSF	Optimum Safety Factor
PBA	Performance-Based Approach
PI	Performance-Based IOSF Approach
PR	Performance-Based ROSF Approach
SCP	Sequential Convex Programming
RBTO	Reliability-Based Topology Optimization
ROSF	Reverse Optimum Safety Factor

References

1. Kharmanda, G.; Olhoff, N. Reliability-Based Topology Optimization /Report N°: 110, Institute of Mechanical Engineering, Aalborg University, Denmark, December 2001.
2. Kharmanda, G.; Olhoff, N. Reliability-Based Topology Optimization as a New Strategy to Generate Different Topologies /In: the Nordic Seminar in Computational Methods, (eds. E. Lund, N. Olhoff and J. Stegmsen), Aalborg University, Denmark, October. 2002, 11-14.
3. Kharmnda, G.; Olhoff, N.; Mohamed, A.; Lemaire, M. Reliability-Based Topology Optimization /Journal of Structural and Multidisciplinary Optimization. 2004, vol. 26, 295–307.
4. Kharmanda, G.; Lambert, S.; Kourdi, N.; Daboul, A.; Elhami, A. Reliability-based topology optimization for different engineering applications /International Journal of CAD/CAM /.2007, 61-69.
5. Patel, J.; Choi, S.K. Classification approach for reliability-based topology optimization using probabilistic neural networks. Structural and Multidisciplinary Optimization. 2012, 45 (4), 529–543.
6. Wang, L.; Liu, D.; Yang, Y.; Wang, X.; Qiu, Z. A novel method of non-probabilistic reliability-based topology optimization corresponding to continuum structures with unknown but bounded uncertainties. Computer Methods in Applied Mechanics and Engineering. 2017, 326, 573-595.

7. Kharmanda, G.; Antypas, I.; Dyachenko, A. Multiobjective shape optimization strategy to increase performance of hollow stems used in artificially replaced hip joints. International Journal of Mechanical Engineering Technology. 2018, 9 (11), 810-820.

8. Kharmanda, G.; Antypas, I.; Dyachenko, A. Inverse Optimum Safety Factor Method for Reliability-Based Topology Optimization Applied to Free Vibrated Structures, Journal of Engineering Technologies and Systems. 2019, 29 (1), 8-19.

9. Kharmanda, G.; Antypas, I.; Dyachenko, A. Effective multiplicative formulation for shape optimization: Optimized Aus-tin-Moore stem for hip prosthesis. International Journal of Mechanical Engineering Technology. 2019, 10 (9), 1-11.

10 Meng, Z.; Pang, Y.; Pu, Y.; Wang, X. New hybrid reliability-based topology optimization method combining fuzzy and probabilistic models for handling epistemic and aleatory uncertainties, Computer Methods in Applied Mechanics and Engineering. 2020, 363, Article 112886

11. Bae, K.; Wang, S. Reliability-based topology optimization /Proceedings of 9th AIAA/ISSMO Symposium on Multidisciplinary Analysis and Optimization. AIAA, 2002, p. 2002-5542.

12. Jung, H-S.; Cho, S.; Yang, Y-S. Reliability-based Robust Topology Design Optimization of Nonlinear Structures, WCSMO5, Italy, 2003.

13. Agarwal, H.; Reliability Based Design Optimization: Formulations and Methodologies /PhD thesis, University of Notre Dame. 2004, p. 136.

14. Patel, N.M.; Agarwal, H.; Tovar, A.; Renaud, J. Reliability based topology optimization using the hybrid cellular automaton method /In 1st AIAA Multidisciplinary Design Optimization Specialist Conference, Austin, Texas. 2005, 18-21.

15. Eom, Y.S.; Yoo, K.S.; Park, J.Y.; Han, S.Y. Reliability-based topology optimization using a standard response surface method for three-dimensional structures, Structural and Multidisciplinary Optimization. 2011, 43 (2), 287–295.

16. Jalalpour, M.; Tootkaboni, M. An efficient approach to reliability-based topology optimization for continua under material uncertainty. Journal of Structural and Multidisciplinary Optimization. 2016, 53, 759-772.

17. Kharmanda, G.; El-Hami, A. Biomechanics: Optimization, Uncertainties and Reliability, ISTE & Wiley, ISBN: 9781786300256, 2017, 254.

18. Sigmund, O.; Maute, K. Topology optimization approaches. Structural and Multidisciplinary Optimization. 2013, 48, 1031–1055.

19. Zhang, W.; Zhu, J.; Gao, T. Topology Optimization in Engineering Structure Design, ISTE & Elsevier 2016, ISBN: 9781785482243, 294.

20. Jain, N.; Bankoti, S.; Saxena, R. Topological Optimization of Isotropic Material using Optimal Criteria Method. International Journal for Research in Emerging Science and Technology. 2015, 2 (2), 41-47.

21. Svanberg, K. The method of moving asymptotes – a new method for structural optimization. International Journal for Numerical Methods in Engineering. 1987, 24, 359-373.

22. Zillober, Ch. A globally convergent version of the method of moving asymptotes. Structural Optimization. 1993, 6, 166-174.

23. Ni, Q.; Zillober, Ch.; Schittkowski, K. Sequential Convex Programming Methods for Solving Large Topology Optimization Problems: Implementation and Computational Results, Journal of Computational Mathematics. 2005, 23(5),

24. Kharmanda, G.; Mulki, H. Two decades review of reliability-based topology optimization developments, Uncertainties and Reliability of Multiphysical Systems, 22-6 (2), October 2022, DOI : 10.21494/ISTE.OP.2022.0884

25. Strömberg, N. Efficient detailed design optimization of topology optimization concepts by using support vector machines and metamodels, Engineering Optimization,2020, 52 (7), 1136-1148.

26. Kuiper, J.H. Numerical optimization of artificial joint designs. Ph.D. thesis, Katholieke Universiteit Nijmegen 1993, p

27. Beaupré, G.S.; Orr, T.E.; Carter, D.R. An approach for time-dependent bone modeling and remodeling-application: a preliminary remodeling simulation. Journal of Orthopaedic Research. 1990, 8 (5), 662–670.

28. Kharmanda, G. Integration of multi-objective structural optimization into cementless hip prosthesis design: Improved Austin-Moore model, Computer Methods in Biomechanics and Biomedical Engineering. 2016, 19 (14), 1557-1566.

29. Shaik, S.A.; Bose, K.; Cherukuri, H.P. A study of durability of hip implant, Materials and Design. 2012, 42, 230–237.

30. Kharmanda, G.; Antypas, I.; Dyachenko, A. Integration of reliability-based topology optimization into biomechanics: Application on hollow stems used in cementless total hip arthroplasty. E3S Web of Conferences 2020, 210 (4).

31. Hayes, A.C.; Träff, E.A.; Sørensen, C.V.; Willems, S.V.; Aage, N.; Sigmund, O.; Whiting, G.L. Topology optimization for structural mass reduction of direct drive electric machines. Sustain. Energy Technol. Assess. accepted/in press, 2023. https://doi.org/10.1016/j.seta.2023.103254.

32. Kharmanda, G.; Mulki, H. Reverse Versus Inverse Optimum Safety Factor Approaches for Reliability-based Topology Optimization, Int J Addit Manuf Struct 2022; 1: 2, https://doi.org/10.53964/ijams.2022002.

33. Kharmanda, G. Additive manufacturing of polylactic acid (PLA) material considering preheating uncertainty effect. Uncertainties Reliab. Multi-Phys. Syst. 2022, 22-6, 1–11, https://doi.org/10.21494/ISTE.OP.2022.0852.

34. Kharmanda, G. A Review on Uncertainty Cases in Additively Manufactured Polylactic Acid Using Fused Filament Fabrication Technique. Int. J. Addit. Manuf. Struct. 2023, 2, 1, https://doi.org/10.53964/ijams.2023001.

35. Myers, D.; Abdel-Wahab, A.; Hafeez, F.; Kovacev, N.; Essa, K. Optimisation of the additive manufacturing parameters of polylactic acid (PLA) cellular structures for biomedical applications. J. Mech. Behav. Biomed. Mater. 2022, 136, 105447. https://doi.org/10.1016/j.jmbbm.2022.105447.

36. Kharmanda, G. Challenges and Future Perspectives for Additively Manufactured Polylactic Acid Using Fused Filament Fabrication in Dentistry. J. Funct. Biomater. 2023, 14, 334. https://doi.org/10.3390/jfb14070334.

